

Potential Energy Surface and State-to-State Dynamics of Chemical Reactions

Ajay Mohan Singh Rawat

Supervisor: Prof. Susanta Mahapatra

School of Chemistry
University of Hyderabad
Telangana 500046, India

Reg. No.: 17CHPH62

PhD viva-voce



<https://github.com/ajaymrawat/>



- 1 **Chapter 1:** Introduction
- 2 **Chapter 2:** Theory and Methodology
- 3 **Chapter 3:** Quantum and classical comparison and Isotopic effect in $\text{H} + \text{LiH}^+ \rightarrow \text{H}_2 + \text{Li}^+$ reaction
- 4 **Chapter 4:** Construction of the global potential energy surface for the ground electronic state of HeLiH^+ system
- 5 **Chapter 5:** State-to-state dynamics of isotopic exchange reaction ${}^{18}\text{O} + {}^{16}\text{O} {}^{16}\text{O} (\nu = 0, j = 1) \rightarrow {}^{18}\text{O} {}^{16}\text{O} + {}^{16}\text{O}$
- 6 **Chapter 6:** Summary and Outlook

Research themes

① Global fitting of potential energy surface (PES)

- Machine learning (ML) methods
- Non-ML methods

① Global fitting of potential energy surface (PES)

- Machine learning (ML) methods
- Non-ML methods

② Adiabatic reaction dynamics studies

- ① Quantum mechanical method
- ② Classical method

Introduction

Chemistry: about physical or chemical changes !!

Introduction

Chemistry: about physical or chemical changes !!

Chemical reaction: transformation of a chemical species from one chemical form to another.

Introduction

Chemistry: about physical or chemical changes !!

Chemical reaction: transformation of a chemical species from one chemical form to another.

... such as: $A + BC \rightarrow AB + C$

Introduction

Chemistry: about physical or chemical changes !!

Chemical reaction: transformation of a chemical species from one chemical form to another.

... such as: $A + BC \rightarrow AB + C$

Different branches of chemistry *mean* different aspects of a reaction.

Introduction

Chemistry: about physical or chemical changes !!

Chemical reaction: transformation of a chemical species from one chemical form to another.

... such as: $A + BC \rightarrow AB + C$

Different branches of chemistry *mean* different aspects of a reaction.

Molecular reaction dynamics deals with the molecular level understanding of a reaction.

Introduction: Molecular reaction dynamics (MRD)

Molecular level understanding: *effect of energy, orientation, etc. of reactant species on the reaction outcomes!*

Molecular level understanding: *effect of energy, orientation, etc. of reactant species on the reaction outcomes!* What motivates these investigations?

① Practical aspect:

- Controlling reaction outcomes.
- Evolution of chemistry.
- High energy applications.

Molecular level understanding: *effect of energy, orientation, etc. of reactant species on the reaction outcomes!* What motivates these investigations?

① Practical aspect:

- Controlling reaction outcomes.
- Evolution of chemistry.
- High energy applications.

② Philosophical aspect:

- True picture of the reality.
- Evolution of the MRD.

Molecular level understanding: *effect of energy, orientation, etc. of reactant species on the reaction outcomes!* What motivates these investigations?

① Practical aspect:

- Controlling reaction outcomes.
- Evolution of chemistry.
- High energy applications.

② Philosophical aspect:

- True picture of the reality.
- Evolution of the MRD.

Approaches: Theoretical and Experimental.

Theoretical approach: Theory and Methodology

In atomic dimensions,

Time-dependent Schrödinger equation:

$$i\hbar \frac{\partial \psi(\vec{r}_e, \vec{r}_N, t)}{\partial t} = \hat{H}\psi(\vec{r}_e, \vec{r}_N, t). \quad (1)$$

Time-independent Schrödinger equation:

$$\hat{H}\psi(\vec{r}_e, \vec{r}_N) = E\psi(\vec{r}_e, \vec{r}_N) \quad (2)$$

Theoretical approach: Theory and Methodology

In atomic dimensions,

Time-dependent Schrödinger equation:

$$i\hbar \frac{\partial \psi(\vec{r}_e, \vec{r}_N, t)}{\partial t} = \hat{H}\psi(\vec{r}_e, \vec{r}_N, t). \quad (1)$$

Time-independent Schrödinger equation:

$$\hat{H}\psi(\vec{r}_e, \vec{r}_N) = E\psi(\vec{r}_e, \vec{r}_N) \quad (2)$$

Here,

$$\hat{H} = - \sum_A \frac{1}{2M_A} \nabla_A^2 - \sum_i \frac{1}{2} \nabla_i^2 - \sum_i \sum_A \frac{Z_A}{r_{iA}} + \sum_i \sum_{j>i} \frac{1}{r_{ij}} + \sum_A \sum_{B>A} \frac{Z_A Z_B}{r_{AB}} \quad (3)$$

Theoretical approach: Theory and Methodology

In atomic dimensions,

Time-dependent Schrödinger equation:

$$i\hbar \frac{\partial \psi(\vec{r}_e, \vec{r}_N, t)}{\partial t} = \hat{H}\psi(\vec{r}_e, \vec{r}_N, t). \quad (1)$$

Time-independent Schrödinger equation:

$$\hat{H}\psi(\vec{r}_e, \vec{r}_N) = E\psi(\vec{r}_e, \vec{r}_N) \quad (2)$$

Here,

$$\hat{H} = - \sum_A \frac{1}{2M_A} \nabla_A^2 - \sum_i \frac{1}{2} \nabla_i^2 - \sum_i \sum_A \frac{Z_A}{r_{iA}} + \sum_i \sum_{j>i} \frac{1}{r_{ij}} + \sum_A \sum_{B>A} \frac{Z_A Z_B}{r_{AB}} \quad (3)$$

Solving the above two equations is not easy, unless we invoke Born-Oppenheimer (BO) approximation!

Theory and Methodology: BO Approximation

Nucleus is heavier than electron! ($m_{nucleus}^H \sim 1836m_e$), consequently:

Theory and Methodology: BO Approximation

Nucleus is heavier than electron! ($m_{nucleus}^H \sim 1836m_e$), consequently:

- ▶ Nuclear and electronic motion: independent.
- ▶ Total wavepacket = product of electronic and nuclear wave functions.

Theory and Methodology: BO Approximation

Nucleus is heavier than electron! ($m_{nucleus}^H \sim 1836m_e$), consequently:

- ▶ Nuclear and electronic motion: independent.
- ▶ Total wavepacket = product of electronic and nuclear wave functions.

Electronic and nuclear parts can be solved independently.

Theory and Methodology: BO Approximation

Nucleus is heavier than electron! ($m_{nucleus}^H \sim 1836m_e$), consequently:

- ▶ Nuclear and electronic motion: independent.
- ▶ Total wavepacket = product of electronic and nuclear wave functions.

Electronic and nuclear parts can be solved independently. Nuclear Schrödinger equation (for j^{th} state):

$$(\hat{T}_N + V_j^{tot} - E)\chi_j(R) - \sum_i \hat{\Lambda}_{ji}\chi_i(R) = 0 \quad (4)$$

Theory and Methodology: BO Approximation

Nucleus is heavier than electron! ($m_{nucleus}^H \sim 1836m_e$), consequently:

- ▶ Nuclear and electronic motion: independent.
- ▶ Total wavepacket = product of electronic and nuclear wave functions.

Electronic and nuclear parts can be solved independently. Nuclear Schrödinger equation (for j^{th} state):

$$(\hat{T}_N + V_j^{tot} - E)\chi_j(R) - \sum_i \hat{\Lambda}_{ji}\chi_i(R) = 0 \quad (4)$$

Here,

$$\hat{\Lambda}_{ji} = \frac{1}{2m}(2\hat{F}_{ji} \cdot \nabla + \hat{G}_{ji})$$

Vector coupling $\hat{F}_{ji} = <\Phi_j(r; R)|\nabla|\Phi_i(r; R)>$

Scalar coupling $\hat{G}_{ji} = <\Phi_j(r; R)|\nabla^2|\Phi_i(r; R)>$

Theory and Methodology: BO Approximation

Nucleus is heavier than electron! ($m_{nucleus}^H \sim 1836m_e$), consequently:

- ▶ Nuclear and electronic motion: independent.
- ▶ Total wavepacket = product of electronic and nuclear wave functions.

Electronic and nuclear parts can be solved independently. Nuclear Schrödinger equation (for j^{th} state):

$$(\hat{T}_N + V_j^{tot} - E)\chi_j(R) - \sum_i \hat{\Lambda}_{ji}\chi_i(R) = 0 \quad (4)$$

Here,

$$\hat{\Lambda}_{ji} = \frac{1}{2m}(2\hat{F}_{ji} \cdot \nabla + \hat{G}_{ji})$$

Vector coupling $\hat{F}_{ji} = <\Phi_j(r; R)|\nabla|\Phi_i(r; R)>$

Scalar coupling $\hat{G}_{ji} = <\Phi_j(r; R)|\nabla^2|\Phi_i(r; R)>$

Eq. 4 is non-adiabatic form. When $\hat{\Lambda}_{ji} = 0$, the adiabatic form is obtained.

$$(\hat{T}_N + V_j^{tot} - E)\chi_j(R) = 0 \quad (5)$$

Theory and Methodology: BO Approximation

Nucleus is heavier than electron! ($m_{nucleus}^H \sim 1836m_e$), consequently:

- ▶ Nuclear and electronic motion: independent.
- ▶ Total wavepacket = product of electronic and nuclear wave functions.

Electronic and nuclear parts can be solved independently. Nuclear Schrödinger equation (for j^{th} state):

$$(\hat{T}_N + V_j^{tot} - E)\chi_j(R) - \sum_i \hat{\Lambda}_{ji}\chi_i(R) = 0 \quad (4)$$

Here,

$$\hat{\Lambda}_{ji} = \frac{1}{2m}(2\hat{F}_{ji} \cdot \nabla + \hat{G}_{ji})$$

Vector coupling $\hat{F}_{ji} = <\Phi_j(r; R)|\nabla|\Phi_i(r; R)>$

Scalar coupling $\hat{G}_{ji} = <\Phi_j(r; R)|\nabla^2|\Phi_i(r; R)>$

Eq. 4 is non-adiabatic form. When $\hat{\Lambda}_{ji} = 0$, the adiabatic form is obtained.

$$(\hat{T}_N + V_j^{tot} - E)\chi_j(R) = 0 \quad (5)$$

Adiabatic dynamics is used in the works presented here!

Theory and Methodology: BO Approximation

Electronic part:

$$\hat{H}_e \Phi_i(r; R) = V_i^{el}(R) \Phi_i(r; R) \quad (6)$$

Theory and Methodology: BO Approximation

Electronic part:

$$\hat{H}_e \Phi_i(r; R) = V_i^{el}(R) \Phi_i(r; R) \quad (6)$$

where,

$$\hat{H}_e = - \sum_i \frac{1}{2} \nabla_i^2 - \sum_i \sum_A \frac{Z_A}{r_{iA}} + \sum_i \sum_{j>i} \frac{1}{r_{ij}}$$

Theory and Methodology: BO Approximation

Electronic part:

$$\hat{H}_e \Phi_i(r; R) = V_i^{el}(R) \Phi_i(r; R) \quad (6)$$

where,

$$\hat{H}_e = - \sum_i \frac{1}{2} \nabla_i^2 - \sum_i \sum_A \frac{Z_A}{r_{iA}} + \sum_i \sum_{j>i} \frac{1}{r_{ij}}$$

Electronic energy $V_i^{tot}(R) = V_i^{el}(R) + \hat{V}_{NN}(R)$ (7)

Theory and Methodology: BO Approximation

Electronic part:

$$\hat{H}_e \Phi_i(r; R) = V_i^{el}(R) \Phi_i(r; R) \quad (6)$$

where,

$$\hat{H}_e = - \sum_i \frac{1}{2} \nabla_i^2 - \sum_i \sum_A \frac{Z_A}{r_{iA}} + \sum_i \sum_{j>i} \frac{1}{r_{ij}}$$

$$\text{Electronic energy } V_i^{tot}(R) = V_i^{el}(R) + \hat{V}_{NN}(R) \quad (7)$$

In configuration space \mathbf{R} $V_i^{tot}(R)$ gives the PES.

Theory and Methodology: BO Approximation

Electronic part:

$$\hat{H}_e \Phi_i(r; R) = V_i^{el}(R) \Phi_i(r; R) \quad (6)$$

where,

$$\hat{H}_e = - \sum_i \frac{1}{2} \nabla_i^2 - \sum_i \sum_A \frac{Z_A}{r_{iA}} + \sum_i \sum_{j>i} \frac{1}{r_{ij}}$$

$$\text{Electronic energy } V_i^{tot}(R) = V_i^{el}(R) + \hat{V}_{NN}(R) \quad (7)$$

In configuration space \mathbf{R} $V_i^{tot}(R)$ gives the PES.

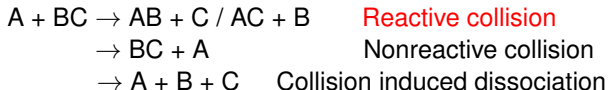
Since electronic structure calculations are expensive, fitting and using the analytical form is the best solution!

Theory and Methodology: Introduction to dynamics

Reaction system in current work: Triatomic reaction system (atom-diatom collision)

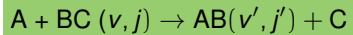
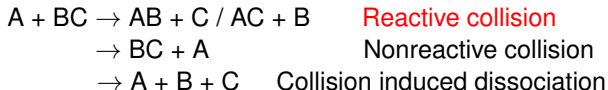
Theory and Methodology: Introduction to dynamics

Reaction system in current work: Triatomic reaction system (atom-diatom collision)



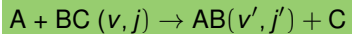
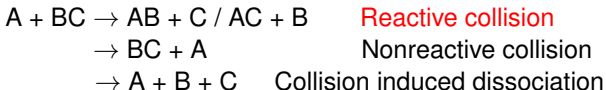
Theory and Methodology: Introduction to dynamics

Reaction system in current work: Triatomic reaction system (atom-diatom collision)



Theory and Methodology: Introduction to dynamics

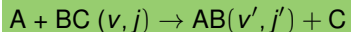
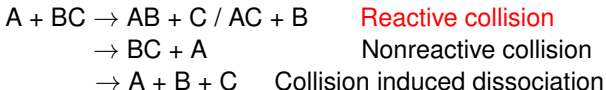
Reaction system in current work: Triatomic reaction system (atom-diatom collision)



- Quantum and classical approaches can be used in theoretical studies.

Theory and Methodology: Introduction to dynamics

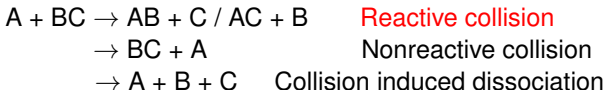
Reaction system in current work: Triatomic reaction system (atom-diatom collision)



- ▶ Quantum and classical approaches can be used in theoretical studies.
- ▶ Quantum methods are relatively more accurate than classical methods.

Theory and Methodology: Introduction to dynamics

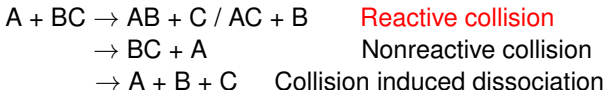
Reaction system in current work: Triatomic reaction system (atom-diatom collision)



- ▶ Quantum and classical approaches can be used in theoretical studies.
- ▶ Quantum methods are relatively more accurate than classical methods.
- ▶ **Equation(s) of motion**
 - **Quantum:** Schrödinger equation
 - **Classical:** Hamilton's equations

Theory and Methodology: Introduction to dynamics

Reaction system in current work: Triatomic reaction system (atom-diatom collision)



- ▶ Quantum and classical approaches can be used in theoretical studies.
- ▶ Quantum methods are relatively more accurate than classical methods.
- ▶ **Equation(s) of motion**
 - **Quantum:** Schrödinger equation
 - **Classical:** Hamilton's equations

QM and Classical both methods are used in our investigations!

Theory and Methodology: QM method

- ▶ Wavepacket methods solve time-dependent Schrödinger equation (TDSE).

Theory and Methodology: QM method

- ▶ Wavepacket methods solve time-dependent Schrödinger equation (TDSE).

$$i\hbar \frac{\partial \psi(\vec{r}_N, t)}{\partial t} = \hat{H}_N \psi(\vec{r}_N, t) \quad (8)$$

Theory and Methodology: QM method

- ▶ Wavepacket methods solve time-dependent Schrödinger equation (TDSE).

$$i\hbar \frac{\partial \psi(\vec{r}_N, t)}{\partial t} = \hat{H}_N \psi(\vec{r}_N, t) \quad (8)$$

$$\psi(\vec{r}_N, t) = \exp\left(\frac{-i\hat{H}_N t}{\hbar}\right) \psi(\vec{r}_N, 0), \quad (9)$$

Theory and Methodology: QM method

- ▶ Wavepacket methods solve time-dependent Schrödinger equation (TDSE).

$$i\hbar \frac{\partial \psi(\vec{r}_N, t)}{\partial t} = \hat{H}_N \psi(\vec{r}_N, t) \quad (8)$$

$$\psi(\vec{r}_N, t) = \exp\left(\frac{-i\hat{H}_N t}{\hbar}\right) \psi(\vec{r}_N, 0), \quad (9)$$

- ▶ Time evolution operator $\exp\left(\frac{-i\hat{H}_N t}{\hbar}\right)$ is approximated using:
 - ➊ Split operator method
 - ➋ Chebyshev polynomial method

Theory and Methodology: QM method

- Wavepacket methods solve time-dependent Schrödinger equation (TDSE).

$$i\hbar \frac{\partial \psi(\vec{r}_N, t)}{\partial t} = \hat{H}_N \psi(\vec{r}_N, t) \quad (8)$$

$$\psi(\vec{r}_N, t) = \exp\left(\frac{-i\hat{H}_N t}{\hbar}\right) \psi(\vec{r}_N, 0), \quad (9)$$

- Time evolution operator $\exp\left(\frac{-i\hat{H}_N t}{\hbar}\right)$ is approximated using:
 - ➊ Split operator method
 - ➋ Chebyshev polynomial method

Eq. 9 is the complex but the one used in the current works is real form.

Theory and Methodology: Classical method

Equations of motion (Hamilton's equation):

$$\frac{\partial q}{\partial t} = \frac{\partial H}{\partial p} = \frac{p}{\mu} \quad (10)$$

$$\frac{\partial p}{\partial t} = -\frac{\partial H}{\partial q} = -\sum_{j=1}^3 \left(\frac{\partial V}{\partial R_j} \right) \left(\frac{\partial R_j}{\partial q_i^r} \right) \quad (11)$$

Theory and Methodology: Classical method

Equations of motion (Hamilton's equation):

$$\frac{\partial q}{\partial t} = \frac{\partial H}{\partial p} = \frac{p}{\mu} \quad (10)$$

$$\frac{\partial p}{\partial t} = -\frac{\partial H}{\partial q} = -\sum_{j=1}^3 \left(\frac{\partial V}{\partial R_j} \right) \left(\frac{\partial R_j}{\partial q_i^r} \right) \quad (11)$$

Numerical approach: Fixed and adaptive step-size *fourth order Runge-Kutta method.*

Theory and Methodology: Classical method

Equations of motion (Hamilton's equation):

$$\frac{\partial q}{\partial t} = \frac{\partial H}{\partial p} = \frac{p}{\mu} \quad (10)$$

$$\frac{\partial p}{\partial t} = -\frac{\partial H}{\partial q} = -\sum_{j=1}^3 \left(\frac{\partial V}{\partial R_j} \right) \left(\frac{\partial R_j}{\partial q_i^r} \right) \quad (11)$$

Numerical approach: Fixed and adaptive step-size *fourth order Runge-Kutta method.*

Form of classical method used:

Quasi classical trajectory (QCT) method: Classical method with quantum approximations.

Theory and Methodology: Reaction observables

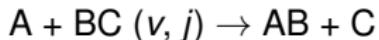
- ① Reaction probability
- ② Integral cross section (ICS)
- ③ Differential cross section (DCS)
- ④ Rate constant

Theory and Methodology: Reaction observables

- ① Reaction probability
- ② Integral cross section (ICS)
- ③ Differential cross section (DCS)
- ④ Rate constant

The observables are calculated at **state-selected** and **state-to-state** levels.

► **State-selected level:**

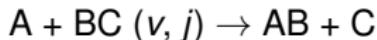


Theory and Methodology: Reaction observables

- ① Reaction probability
- ② Integral cross section (ICS)
- ③ Differential cross section (DCS)
- ④ Rate constant

The observables are calculated at **state-selected** and **state-to-state** levels.

► **State-selected level:**



► **State-to-state level:**



Theory and Methodology: PES fitting

$$\text{Electronic energy } V_i^{tot}(R) = V_i^{el}(R) + \hat{V}_{NN}(R) \quad (12)$$

For a triatomic system: $V_{ABC}^{tot}(r_{AB}, r_{BC}, r_{AC})$

Theory and Methodology: PES fitting

$$\text{Electronic energy } V_i^{tot}(R) = V_i^{el}(R) + \hat{V}_{NN}(R) \quad (12)$$

For a triatomic system: $V_{ABC}^{tot}(r_{AB}, r_{BC}, r_{AC})$: four-dimensional global surface
 $\hat{V}_{el}(R)\phi_e(r; R) = (\hat{T}_{e^-} + \hat{V}_{Ne^-} + \hat{V}_{e^-e^-} + \hat{V}_{NN})\phi(r; R)$

Theory and Methodology: PES fitting

$$\text{Electronic energy } V_i^{tot}(R) = V_i^{el}(R) + \hat{V}_{NN}(R) \quad (12)$$

For a triatomic system: $V_{ABC}^{tot}(r_{AB}, r_{BC}, r_{AC})$: four-dimensional global surface

$$\hat{V}_{el}(R)\phi_e(r; R) = (\hat{T}_{e^-} + \hat{V}_{Ne^-} + \hat{V}_{e^-e^-} + \hat{V}_{NN})\phi(r; R)$$

- ▶ First principle energy calculations are **expensive!!**
- ▶ Using an analytical formula is fast and reasonably accurate.
- ▶ PES fitting has two parts:
 - Generating ab initio energy points.
 - Fitting energy points with analytical function.

The two parts are equally important!

Theory and Methodology: PES fitting

$$\text{Electronic energy } V_i^{tot}(R) = V_i^{el}(R) + \hat{V}_{NN}(R) \quad (12)$$

For a triatomic system: $V_{ABC}^{tot}(r_{AB}, r_{BC}, r_{AC})$: four-dimensional global surface

$$\hat{V}_{el}(R)\phi_e(r; R) = (\hat{T}_{e^-} + \hat{V}_{Ne^-} + \hat{V}_{e^-e^-} + \hat{V}_{NN})\phi(r; R)$$

- ▶ First principle energy calculations are **expensive!!**
- ▶ Using an analytical formula is fast and reasonably accurate.
- ▶ PES fitting has two parts:
 - Generating ab initio energy points.
 - Fitting energy points with analytical function.
The two parts are equally important!
- ▶ **Generating energy points involve:**
 - Choice of electronic structure methods.
 - Choice of coordinate grids.

Theory and Methodology: Fitting with analytical function

- ▶ Representing the potential
 - Many-body expansion (MBE)¹
 - Double many-body expansion
 - Global representation

¹ *Molecular Physics*, **29**(5):1387–1407, 1975.

Theory and Methodology: Fitting with analytical function

- ▶ Representing the potential
 - Many-body expansion (MBE)¹
 - Double many-body expansion
 - Global representation

MBE and DMBE represent the total potential as fragments.

¹ *Molecular Physics*, **29**(5):1387–1407, 1975.

Theory and Methodology: Fitting with analytical function

► Representing the potential

- Many-body expansion (MBE)¹
- Double many-body expansion
- Global representation

MBE and DMBE represent the total potential as fragments.

► Many-body expansion (MBE):

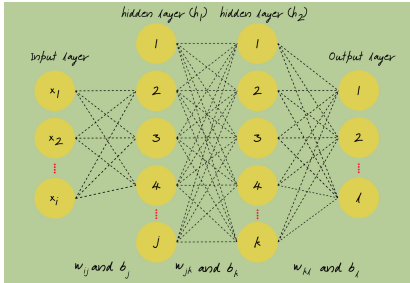
$$V_{ABC}^{tot, MBE}(r_{AB}, r_{BC}, r_{AC}) = \sum_i V_i^{(1)} + \sum_j V^{(2)}(r_j) + V^{(3)}(r_{AB}, r_{BC}, r_{AC}) \quad (13)$$

$$\sum_i V_i^{(1)} = V_A^{(1)} + V_B^{(1)} + V_C^{(1)}$$

$$\sum_j V_j^{(2)}(r_j) = V_{AB}^{(2)}(r_{AB}) + V_{BC}^{(2)}(r_{BC}) + V_{AC}^{(2)}(r_{AC})$$

¹ Molecular Physics, 29(5):1387–1407, 1975.

Theory and Methodology: ML method



► Neural network (NN)

- Hyperparameters: No. of neurons and layers, learning rate, etc., affect the training.
- Overfitting and underfitting are the primary bottlenecks.

NN function (with one neuron in the output layer):

$$V^{\text{NN}} = b^{(3)} + \sum_{k=1}^{N_k} w_k^{(3)} f^{(2)} \left[b_k^{(2)} + \sum_{j=1}^{N_j} w_{jk}^{(2)} f^{(1)} \left(b_j^{(1)} + w_{ij}^{(1)} G_i \right) \right] \quad (14)$$

The ML method cares about the numbers without knowing the origin of the behavior of them!

Data should **best** represent the global configuration space of the molecular system.

Theory and Methodology: Non ML method

- Aguado form:¹

¹ *J. Chem. Phys.* **96**, 1265–1275, 1992.

Theory and Methodology: Non ML method

► Aguado form:¹

Two-body part:

$$V_{AB}^{(2)}(R_{AB}) = \frac{c_0 e^{-\alpha_{AB} R_{AB}}}{R_{AB}} + \sum_{i=1}^N c_i \rho_{AB}^i \quad (15)$$

$$\rho_{AB} = R_{AB} e^{-\beta_{AB}^{(2)} R_{AB}}$$

Three-body part:

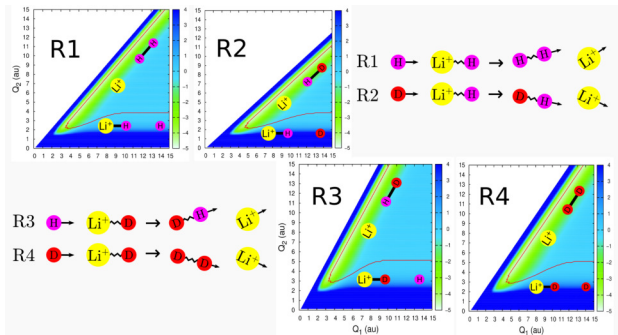
$$V_{ABC}^{(3)} = \sum_{ijk=1}^M d_{ijk} \rho_{AB}^i \rho_{BC}^j \rho_{AC}^k . \quad (16)$$

$$i + j + k \neq i \neq j \neq k \text{ and } i + j + k \leq M$$

¹ J. Chem. Phys. **96**, 1265–1275, 1992.

Chapter 3

Quantum and classical comparison and Isotopic effect in $H + LiH^+ \rightarrow H_2 + Li^+$ reaction^{1 2 3}



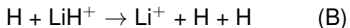
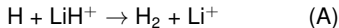
¹J. Phys. Chem. A **127**, 51, 10733 (2023).

²J. Phys. Chem. A **125**, 16, 3387 (2021).

³Phys. Chem. Chem. Phys. **23**, 27327 (2021).

Introduction and Motivation

- ▶ **Early universe:** Li, H, He, and D.
- ▶ **LiHe⁺ and LiH⁺:** possible molecular forms of Li in early universe.
- ▶ Destruction and formation of these molecular species: important reaction events.
- ▶ **Motivation:** possible collision of LiH⁺ with abundant H atoms.
- ▶ **Examples:**



A: Exchange reaction. **B:** Collision-induced dissociation.

The reaction considered in the present work:



Research themes

- ① Comparison of quantum and classical methods
- ② Study of the isotopic effect

¹J. Chem. Phys. **119**, 11241 (2003).

²J. Phys. Chem. A **125**, 16, 3387 (2021).

Research themes

- ① Comparison of quantum and classical methods
- ② Study of the isotopic effect

PES: Martinazzo et al.¹

Theoretical methodology: QCT-HB/GB methods

¹J. Chem. Phys. **119**, 11241 (2003).

²J. Phys. Chem. A **125**, 16, 3387 (2021).

Research themes

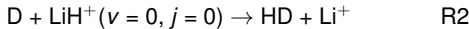
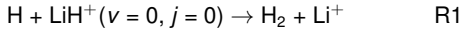
- ① Comparison of quantum and classical methods
- ② Study of the isotopic effect

PES: Martinazzo et al.¹

Theoretical methodology: QCT-HB/GB methods

Comparison of quantum and classical methods

Reactions considered:

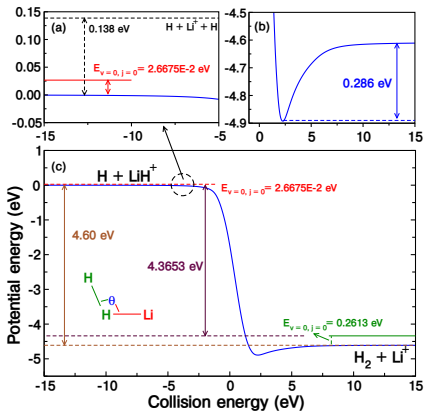


Note: QM results from earlier² & QCT results from current work.

¹J. Chem. Phys. **119**, 11241 (2003).

²J. Phys. Chem. A **125**, 16, 3387 (2021).

$\text{H} + \text{LiH}^+ \rightarrow \text{H}_2 + \text{Li}^+$ reaction: A brief introduction



- **Exoergicity:** ~4.60 eV (without ZPE) and ~4.36 eV (with ZPE of reactant and product diatoms)
- CID opens at ~0.138 eV.
- **Shallow minima:** ~0.286 eV below product asymptote.

QM and QCT comparison: Total reaction probability

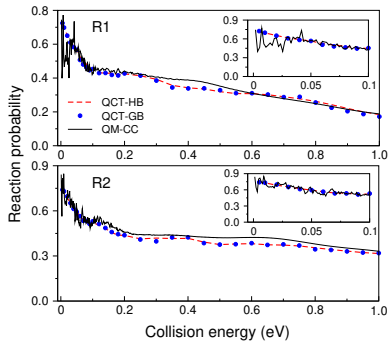


Figure 1: Total reaction probability at $J=0$.

QM and QCT comparison: Total reaction probability

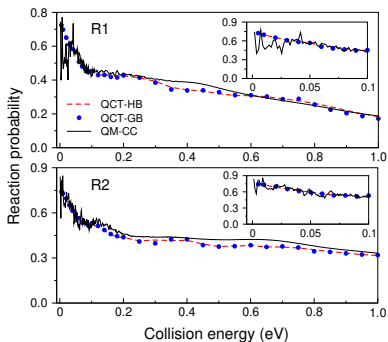


Figure 1: Total reaction probability at $J=0$.

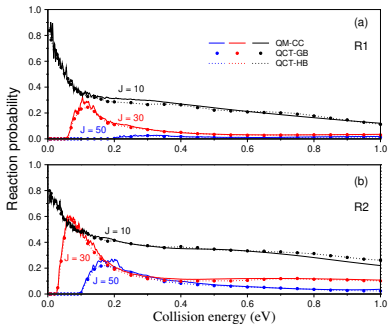


Figure 2: Total reaction probability at different J values.

QM and QCT comparison: ICS

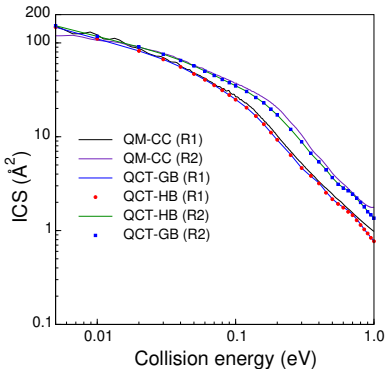
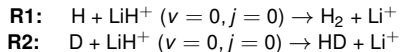


Figure 3: Initial state-selected QM and QCT ICSs for R1 and R2.



- ▶ ICS decreases with increasing collision energy: *typical barrierless exoergic reaction behavior.*
- ▶ QCT-GB/HB and QM ICSs are following each other.
- ▶ QM shows resonance structure which are not available in QCT ICS.

QM and QCT comparison: DCS

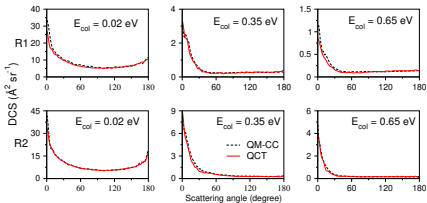


Figure 4: QCT DCSs for R1 and R2.

- DCS is forward bias, suggesting a direct mechanism.
- At low collision energy, backward scattering is observed.

QM and QCT comparison: DCS

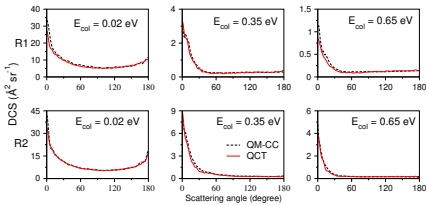


Figure 4: QCT DCSs for R1 and R2.

- DCS is forward bias, suggesting a direct mechanism.
- At low collision energy, backward scattering is observed.

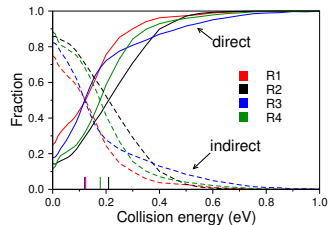


Figure 5: Fraction of indirect and direct trajectories for R1 and R2.

QM and QCT comparison: Rate constants

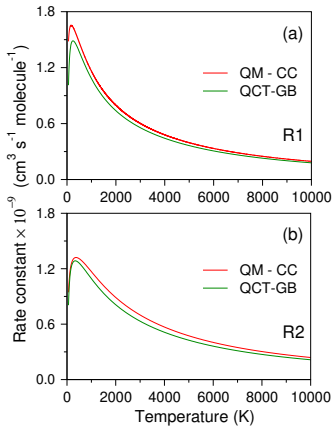
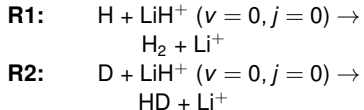


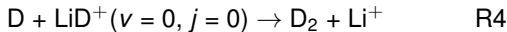
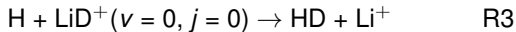
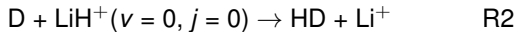
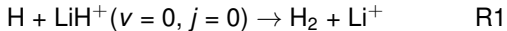
Figure 6: State-selected rate constants for ($v=0, j=0$) initial state of reactant diatom.



- Rate constants are shown up to 10000 K.
- Rate constant increases first and decreases later.
- The QM and QCT rate constants agree with each other.

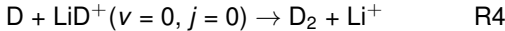
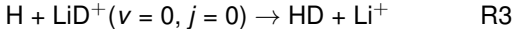
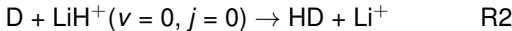
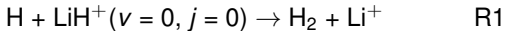
Part 2 : Isotopic effect

Reactions considered in the study of isotopic effect:



Part 2 : Isotopic effect

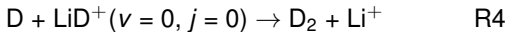
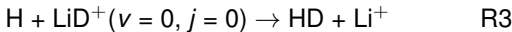
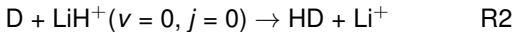
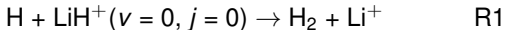
Reactions considered in the study of isotopic effect:



Only QCT methods are used for isotopic effect investigation. Why?

Part 2 : Isotopic effect

Reactions considered in the study of isotopic effect:



Only QCT methods are used for isotopic effect investigation. Why?

Good agreement between QCT and QM results for R1 and R2, increases the confidence in the accuracy of QCT method.

Isotopic effect ?

Isotopic effect: *change in the reaction dynamics or observables by replacing the isotopic variant in a reaction.*

Isotopic effect ?

Isotopic effect: *change in the reaction dynamics or observables by replacing the isotopic variant in a reaction.*

How do isotopes affect the dynamics of a reaction?

- ▶ Changing the isotopes is changing the masses of the nuclei taking part in the reaction.
- ▶ The adiabatic electronic potentials for the isotopic variants remain the same. However, the forces change as the masses are different.

Isotopic effect ?

Isotopic effect: *change in the reaction dynamics or observables by replacing the isotopic variant in a reaction.*

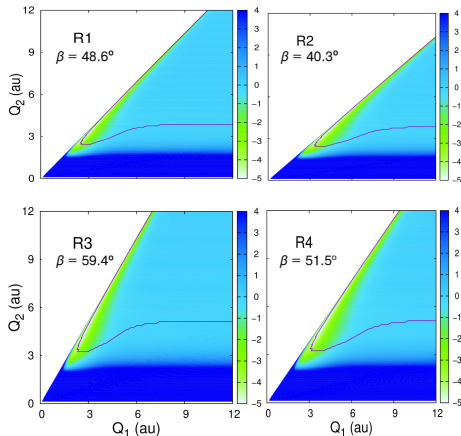
How do isotopes affect the dynamics of a reaction?

- ▶ Changing the isotopes is changing the masses of the nuclei taking part in the reaction.
- ▶ The adiabatic electronic potentials for the isotopic variants remain the same. However, the forces change as the masses are different.

The PESs remain the same for different isotopic variants but are perceived differently!

Is there a way to observe the effect of isotopes on the potential surface?
Possibly, yes! Mass-weighted PES.

Isotopic effect: Mass-weighted PES



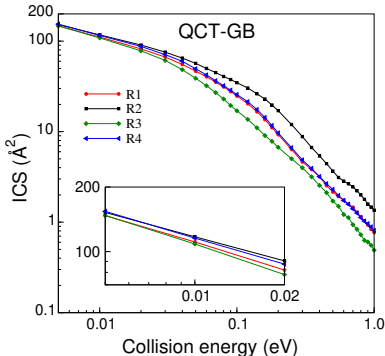
The reactant and product asymptote
are skewed for different isotopic
variants.

Skewness: R2>R1~R4>R3

*Skewness is correlated with the
reaction observables!!*

Figure 7: Contour map of the mass-weighted PESs and MEPs
(shown as a violet-colored line) at an attacking angle ($\angle H_AH_BLi$).

Isotopic effect on ICS



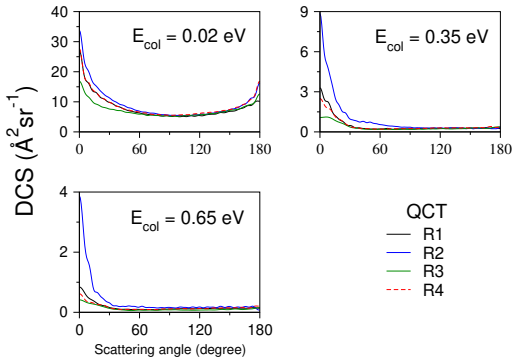
R1: $\text{H} + \text{LiH}^+$ **R2:** $\text{D} + \text{LiH}^+$
R3: $\text{H} + \text{LiD}^+$ **R4:** $\text{D} + \text{LiD}^+$

Order of ICS: $\text{R2} > \text{R1} \sim \text{R4} > \text{R3}$

Skewness: $\text{R2} > \text{R1} \sim \text{R4} > \text{R3}$

Figure 8: Initial state-selected QCT ICSs for R1, R2, R3, and R4.

Isotopic effect on DCS



R1: H + LiH⁺ **R2:** D + LiH⁺
R3: H + LiD⁺ **R4:** D + LiD⁺

- ▶ Isotopic effect is quantitative.
- ▶ The quantitative order of DCS: correlated with the skewness.

Figure 9: Initial state-selected QCT DCSs for R1, R2, R3, and R4.

Chapter 3: Conclusion

QM and QCT comparison:

- ▶ Good agreement at state-selected and state-to-state level.
 - ▶ Scalar and vector observables both are in good agreement.
-

Chapter 3: Conclusion

QM and QCT comparison:

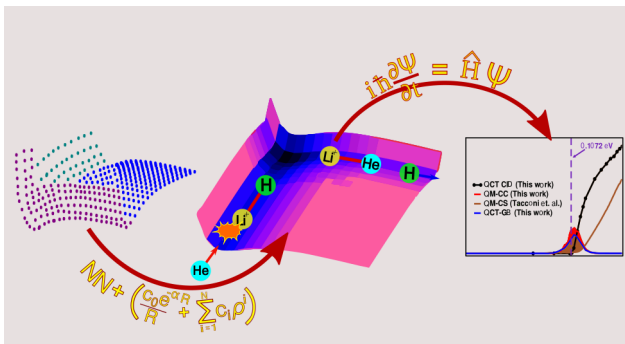
- ▶ Good agreement at state-selected and state-to-state level.
- ▶ Scalar and vector observables both are in good agreement.

Isotopic effect:

- ▶ The treatment of different isotopic variants can be visualised in mass-weighted PES.
- ▶ Significant isotopic effect observed.
- ▶ Isotopic effect: correlated with the skewness of the reactant-product channels.

Chapter 4

Construction of the global potential energy surface for the ground electronic state of HeLiH⁺ system and dynamics of He + LiH⁺ → LiHe⁺ + H reaction¹



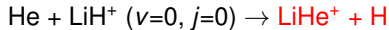
¹J. Chem. Phys. **161**, 124308 (2024).

Introduction and Motivation

- ▶ Li is one of the elements present in the early universe.
- ▶ LiH^+ is possible diatomic form of Li.
- ▶ **Motivation:** possibility of He and LiH^+ collision.
- ▶ Ground electronic state of LiHeH^+ facilitates the following reactions:
 - $\text{He} + \text{LiH}^+ \rightarrow \text{LiHe}^+ + \text{H}$ or $\text{Li}^+ + \text{He} + \text{H}$
 - $\text{H} + \text{LiHe}^+ \rightarrow \text{LiH}^+ + \text{He}$ or $\text{Li}^+ + \text{He} + \text{H}$

Introduction and Motivation

- ▶ Li is one of the elements present in the early universe.
- ▶ LiH^+ is possible diatomic form of Li.
- ▶ **Motivation:** possibility of He and LiH^+ collision.
- ▶ Ground electronic state of LiHeH^+ facilitates the following reactions:
 - $\text{He} + \text{LiH}^+ \rightarrow \text{LiHe}^+ + \text{H}$ or $\text{Li}^+ + \text{He} + \text{H}$
 - $\text{H} + \text{LiHe}^+ \rightarrow \text{LiH}^+ + \text{He}$ or $\text{Li}^+ + \text{He} + \text{H}$
- ▶ Reaction considered in current work:



Brief literature summary and way forward ...

- ▶ Only one PES (Wernli et al.¹) is available. Method: MRCI
- ▶ Only report (Tacconi et al.²) on the dynamics: $\text{He} + \text{LiH}^+ \rightarrow \text{LiHe}^+ + \text{H}$ and $\text{H} + \text{LiHe}^+ \rightarrow \text{LiH}^+ + \text{He}$
- ▶ Results of Tacconi et al. used in assessment of LiHe^+ (Bovino et al.³) in early universe.

¹Int. J. Mass Spectrom. **280**, 57 (2009).

²Phys. Chem. Chem. Phys. **14**, 673 (2012).

³Astrophys. J **19**, 752 (2012).

Brief literature summary and way forward ...

- ▶ Only one PES (Wernli et al.¹) is available. Method: MRCI
- ▶ Only report (Tacconi et al.²) on the dynamics: $\text{He} + \text{LiH}^+ \rightarrow \text{LiHe}^+ + \text{H}$ and $\text{H} + \text{LiHe}^+ \rightarrow \text{LiH}^+ + \text{He}$
- ▶ Results of Tacconi et al. used in assessment of LiHe^+ (Bovino et al.³) in early universe.

Earlier dynamical results doesn't follow the usual trend,
suggesting a possible error!!

¹Int. J. Mass Spectrom. **280**, 57 (2009).

²Phys. Chem. Chem. Phys. **14**, 673 (2012).

³Astrophys. J **19**, 752 (2012).

Brief literature summary and way forward ...

- ▶ Only one PES (Wernli et al.¹) is available. Method: MRCI
- ▶ Only report (Tacconi et al.²) on the dynamics: $\text{He} + \text{LiH}^+ \rightarrow \text{LiHe}^+ + \text{H}$ and $\text{H} + \text{LiHe}^+ \rightarrow \text{LiH}^+ + \text{He}$
- ▶ Results of Tacconi et al. used in assessment of LiHe^+ (Bovino et al.³) in early universe.

Earlier dynamical results doesn't follow the usual trend,
suggesting a possible error!!

Current study?

- ▶ New dynamics results.
- ▶ Constructing HeLiH^+ surface using high level data point.

¹Int. J. Mass Spectrom. **280**, 57 (2009).

²Phys. Chem. Chem. Phys. **14**, 673 (2012).

³Astrophys. J **19**, 752 (2012).

Construction of PES: Representing the potential of HeLiH⁺

Many body expansion (MBE)¹ is used to represent the PES.

$$V_{\text{LiHeH}^+}^{\text{tot,MBE}}(r_{\text{LiH}^+}, r_{\text{LiHe}^+}, r_{\text{HeH}}) = \sum_i V_i^{(1)} + \sum_j V^{(2)}(r_j) + V^{(3)}(r_{\text{LiH}^+}, r_{\text{LiHe}^+}, r_{\text{HeH}}) \quad (17)$$

$$\sum_i V_i^{(1)} = V_{\text{Li}^+}^{(1)} + V_{\text{He}}^{(1)} + V_{\text{H}}^{(1)} = 0$$

$$\sum_j V_j^{(2)}(r_j) = V_{\text{LiH}^+}^{(2)}(r_{\text{LiH}^+}) + V_{\text{LiHe}^+}^{(2)}(r_{\text{LiHe}^+}) + V_{\text{HeH}}^{(2)}(r_{\text{HeH}})$$

¹ Molecular Physics, 29(5):1387–1407, 1975.

Construction of PES: Generating ab initio data and fitting methods

Generating ab initio data:

- ▶ **Grid:** Two bond distances (r_{HeLi^+} and r_{LiH^+}) and bond angle between these (θ).
 - ▶ **Electronic structure calculation:** Full configuration interaction (FCI) method + aug-ccpVQZ basis + extrapolation to CBS limit.
-

Construction of PES: Generating ab initio data and fitting methods

Generating ab initio data:

- ▶ **Grid:** Two bond distances (r_{HeLi^+} and r_{LiH^+}) and bond angle between these (θ).
- ▶ **Electronic structure calculation:** Full configuration interaction (FCI) method + aug-ccpVQZ basis + extrapolation to CBS limit.

Fitting method:

- ▶ **Two-body part:** Neural Network (NN) algorithm + Aguado Paniagua (AP) form. **AP:** HeH, **NN:** LiHe⁺ and LiH⁺
- ▶ **Three-body part:** AP
- ▶ **Optimization algorithm:** Levenberg-Marquardt (LM)

Fitting errors for two-body and three-body parts

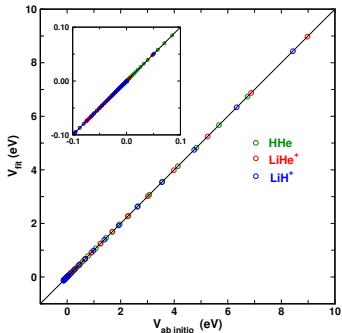


Figure 10: Fitted vs ab initio energy plot for diatoms.

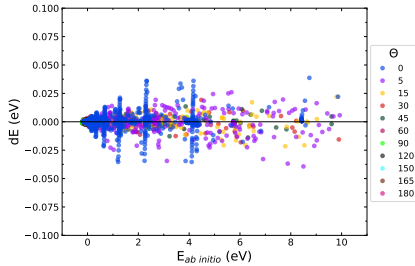


Figure 11: Fitting error ($E_{fit} - E_{ab\ initio}$) at each ab initio data point for overall fitting of LiHeH^+ system.

Root mean square error (RMSE) of fitting:

Two-body (LiHe⁺, LiH⁺, and HeH)
Three-body
Overall

1.04E-04 eV, 3.4E-05 eV, and 9.8E-06 eV
1.63E-03 eV (data < 10.0 eV)
9.28E-04 eV (data < 2.0 eV)

Potential energy curves

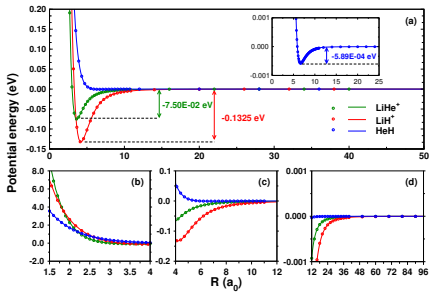


Figure 12: Fitted vs ab initio potential energy curves for diatoms.

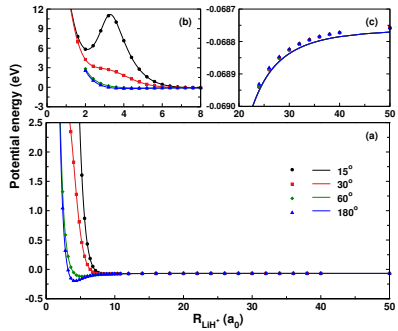


Figure 13: Fitted vs ab initio potential cuts when LiHe⁺ is fixed at 3.40 a_0 .

Fitted and ab initio potential energy surfaces

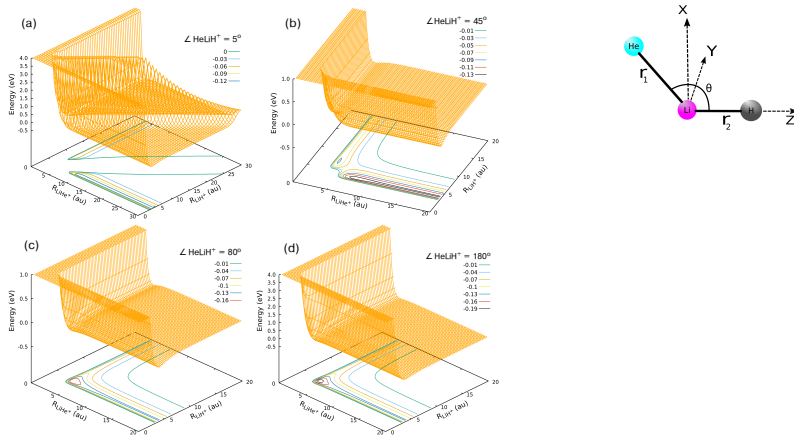


Figure 14: PESs at different attacking angles ($\angle \text{HeLiH}^+$).

Fitted and ab initio potential energy surfaces

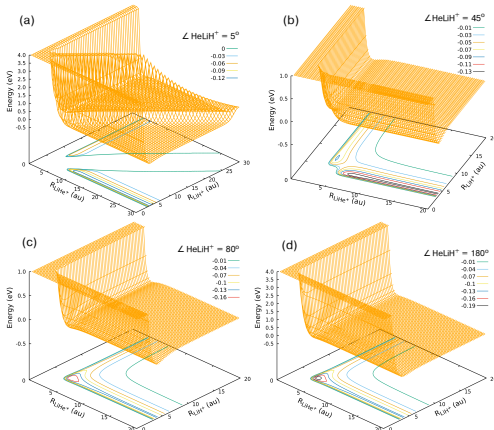


Figure 14: PESs at different attacking angles ($\angle \text{HeLiH}^+$).

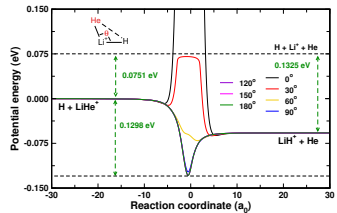
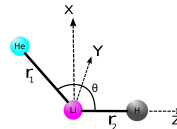
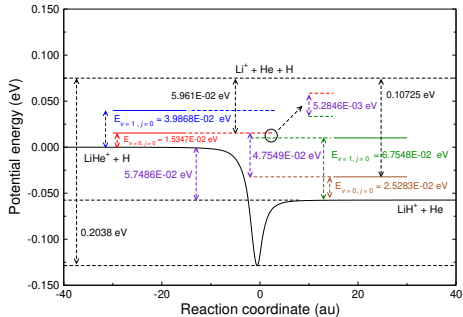


Figure 15: MEPs at different attacking angles ($\angle \text{HeLiH}^+$).

Energetics



- ▶ R1: $\text{H} + \text{LiHe}^+ \rightarrow \text{LiH}^+ + \text{He}$
- ▶ R2: $\text{He} + \text{LiH}^+ \rightarrow \text{LiHe}^+ + \text{H}$
- ▶ Collision induced dissociation (CID):
$$\text{He} + \text{LiH}^+ \rightarrow \text{Li}^+ + \text{He} + \text{H}$$

A little more about (R2)= $\text{He} + \text{LiH}^+ \rightarrow \text{LiHe}^+ + \text{H}$...

- ▶ $\Delta E = 4.7549\text{E-}02 \text{ eV}$ (including ZPE). Endoergic.
- ▶ CID opens at 0.10725 eV.

Methodology

For reaction R2, CID opens at a very low collision energy of ~0.1075 eV, affecting the dynamics of the reaction!

Theoretical methods:

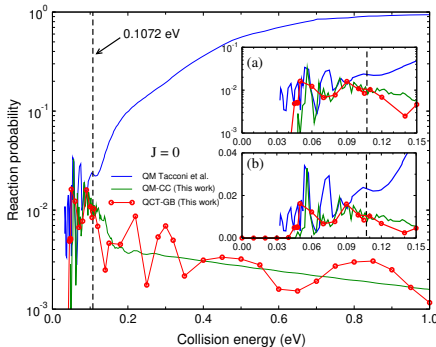
① TDQM

involves the convergence of input parameters, calculations of S-matrix elements for different total angular momentum (J) collisions, and calculations of reaction observables.

② QCT

involves the convergence of b_{max} values, running trajectories, and calculations of reaction observables.

Results: Reaction probabilities



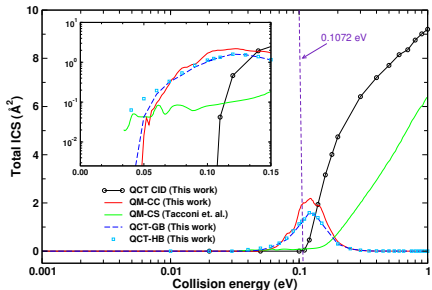
- QM and QCT-GB results increase till ~ 0.1072 eV and then decrease with collision energy.
- Results from Tacconi et al.¹ keep increasing even after the opening of CID.

Figure 16: Reaction probability at $J = 0$ for $\text{He} + \text{LiH}^+$
($v=0, j=0$) $\rightarrow \text{LiHe}^+ + \text{H}$ reaction.

¹ Phys. Chem. Chem. Phys. 14, 673 (2012).

Integral cross section (ICS)

How does the CID affect the reactivity of a reaction?



- ▶ QM-CC and QCT ICSs from our work are compared with QM-CS ICS of Tacconi et al.¹
- ▶ QCT ICS for CID channel from our work is also shown.
- ▶ **Effect of the CID channel is evident!**

Figure 17: ICSs for $\text{He} + \text{LiH}^+ (v=0, j=0) \rightarrow \text{LiHe}^+ + \text{H}$ reaction

¹ Phys. Chem. Chem. Phys. 14, 673 (2012).

State-specific rate constants

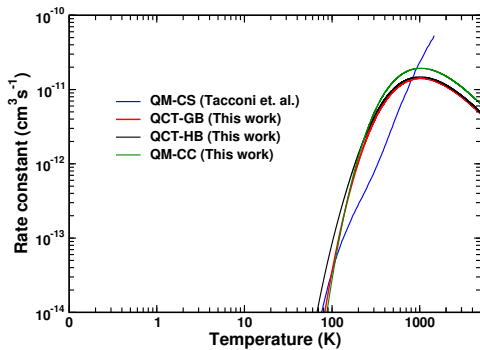


Figure 18: State-specific rate constant for $\text{He} + \text{LiH}^+$
 $(v=0, j=0) \rightarrow \text{LiHe}^+ + \text{H}$ reaction.

- QM-CC and QCT, both rate constants, are calculated in our work.
- The state-specific rate constants from our work are compared with the results of Tacconi et al.¹

¹ Phys. Chem. Chem. Phys. 14, 637 (2012).

Conclusion

Fitting of PES:

¹Phys. Chem. Chem. Phys. 14, 673 (2012).

Conclusion

Fitting of PES:

- ▶ A new global PES was constructed.
 - ▶ Data points: generated at the FCI level of theory, much higher than the earlier surface.
 - ▶ Overall RMSE: 14.21 cm^{-1} (data $\leq 10 \text{ eV}$) and 7.48 cm^{-1} (data $\leq 2 \text{ eV}$).
 - ▶ Neural network and Aguado fitting forms were used in combination.
-

Conclusion

Fitting of PES:

- ▶ A new global PES was constructed.
- ▶ Data points: generated at the FCI level of theory, much higher than the earlier surface.
- ▶ Overall RMSE: 14.21 cm^{-1} (data $\leq 10 \text{ eV}$) and 7.48 cm^{-1} (data $\leq 2 \text{ eV}$).
- ▶ Neural network and Aguado fitting forms were used in combination.

Dynamics of the reaction:

Conclusion

Fitting of PES:

- ▶ A new global PES was constructed.
- ▶ Data points: generated at the FCI level of theory, much higher than the earlier surface.
- ▶ Overall RMSE: 14.21 cm^{-1} (data $\leq 10 \text{ eV}$) and 7.48 cm^{-1} (data $\leq 2 \text{ eV}$).
- ▶ Neural network and Aguado fitting forms were used in combination.

Dynamics of the reaction:

- ▶ Dynamics of $\text{He} + \text{LiH}^+ \rightarrow \text{LiHe}^+ + \text{H}$ is investigated using QM and QCT method.
- ▶ The reaction observables show the effect of the opening of the CID channel at 0.1075 eV.
- ▶ Our results show a different trend than the results of Tacconi et al.¹ reported earlier.

¹ Phys. Chem. Chem. Phys. 14, 673 (2012).

Chapter 5

State-to-state dynamics of isotopic exchange reaction $^{18}\text{O} + ^{16}\text{O}^{16}\text{O} (\nu = 0, j = 1) \rightarrow ^{18}\text{O}^{16}\text{O} + ^{16}\text{O}^1$

¹manuscript under preparation.

Introduction

Introduction

Historically, major interest in this reaction comes from the importance of O₃

Introduction

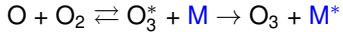
Historically, major interest in this reaction comes from the importance of O₃

- ▶ O₃ is an important atmospheric gas.
- ▶ **Mass-independent fractionation** leading to enrichment of heavier isotope was observed in O₃ (1980-83).

Introduction

Historically, major interest in this reaction comes from the importance of O₃

- ▶ O₃ is an important atmospheric gas.
- ▶ Mass-independent fractionation leading to enrichment of heavier isotope was observed in O₃ (1980-83).
- ▶ One of the mechanisms of O₃ formation is Lindemann mechanism:



Introduction

Historically, major interest in this reaction comes from the importance of O₃

- ▶ O₃ is an important atmospheric gas.
- ▶ Mass-independent fractionation leading to enrichment of heavier isotope was observed in O₃ (1980-83).
- ▶ One of the mechanisms of O₃ formation is Lindemann mechanism:



- ▶ Isotopic exchange reaction (^aO + ^bO^cO → O₃^{*} → ^bO + ^aO^cO) competes with the O₃ formation.
- ▶ Combination of different isotopes: key to understand MIF.

Brief literature summary: Where do we stand?

- ▶ Many PESs have been constructed over the years! (2001-2017 and so on)

¹J. Chem. Phys. 142, 17, 174311 (2015).

²J. Chem. Phys. 142, 17 , 174312 (2015).

³J. Phys. Chem. Lett. 9, 8, 1931 (2018).

⁴J. Chem. Phys. 139, 134307, (2013).

⁵Chem. Phys. Lett. 776, 138648, (2021).

Brief literature summary: Where do we stand?

- ▶ Many PESs have been constructed over the years! (2001-2017 and so on)



¹J. Chem. Phys. 142, 17, 174311 (2015).

²J. Chem. Phys. 142, 17 , 174312 (2015).

³J. Phys. Chem. Lett. 9, 8, 1931 (2018).

⁴J. Chem. Phys. 139, 134307, (2013).

⁵Chem. Phys. Lett. 776, 138648, (2021).

Brief literature summary: Where do we stand?

- ▶ Many PESs have been constructed over the years! (2001-2017 and so on)



Despite the considerable investigations: mismatch between experimental and theoretical data remaineduntil...

¹J. Chem. Phys. 142, 17, 174311 (2015).

²J. Chem. Phys. 142, 17 , 174312 (2015).

³J. Phys. Chem. Lett. 9, 8, 1931 (2018).

⁴J. Chem. Phys. 139, 134307, (2013).

⁵Chem. Phys. Lett. 776, 138648, (2021).

Brief literature summary: Where do we stand?

- ▶ Many PESs have been constructed over the years! (2001-2017 and so on)



Despite the considerable investigations: mismatch between experimental and theoretical data remained**until...**

- ▶ **2015:** TI dynamical study of Rajagopala et al.¹ and Guo et al.² on DLLG PES. *Negative temp. dependence of thermal rate constant observed.*
- ▶ **2017:** First exact match of theoretical and experimental data. Guillon et al.³ (Reaction: 8+66. PES: Tyuterev et al.⁴)

Reason for the mismatch in earlier investigations: An error in the form of a submerged barrier.

¹J. Chem. Phys. 142, 17, 174311 (2015).

²J. Chem. Phys. 142, 17 , 174312 (2015).

³J. Phys. Chem. Lett. 9, 8, 1931 (2018).

⁴J. Chem. Phys. 139, 134307, (2013).

⁵Chem. Phys. Lett. 776, 138648, (2021).

Brief literature summary: Where do we stand?

- ▶ Many PESs have been constructed over the years! (2001-2017 and so on)



Despite the considerable investigations: mismatch between experimental and theoretical data remaineduntil...

- ▶ **2015:** TI dynamical study of Rajagopala et al.¹ and Guo et al.² on DLLG PES. *Negative temp. dependence of thermal rate constant observed.*
- ▶ **2017:** First exact match of theoretical and experimental data. Guillon et al.³ (Reaction: 8+66. PES: Tyuterev et al.⁴)

Reason for the mismatch in earlier investigations: An error in the form of a submerged barrier.

- ▶ **2021:** Korutla et al.⁵: State-to-state DCS and ICSs reported.

¹J. Chem. Phys. 142, 17, 174311 (2015).

²J. Chem. Phys. 142, 17 , 174312 (2015).

³J. Phys. Chem. Lett. 9, 8, 1931 (2018).

⁴J. Chem. Phys. 139, 134307, (2013).

⁵Chem. Phys. Lett. 776, 138648, (2021).

Current study?

What else is left?

Current study?

What else is left?

Motivation:

- ▶ Reporting detailed account of reaction mechanism at the state-to-state level.
-

Current study?

What else is left?

Motivation:

- ▶ Reporting detailed account of reaction mechanism at the state-to-state level.
-

Theoretical methodology:

- ▶ TDWP method in energy range: 0.0 eV - 0.1 eV.
 - ▶ Only 8+66 isotopic variant of the reaction is investigated.
-

Current study?

What else is left?

Motivation:

- ▶ Reporting detailed account of reaction mechanism at the state-to-state level.
-

Theoretical methodology:

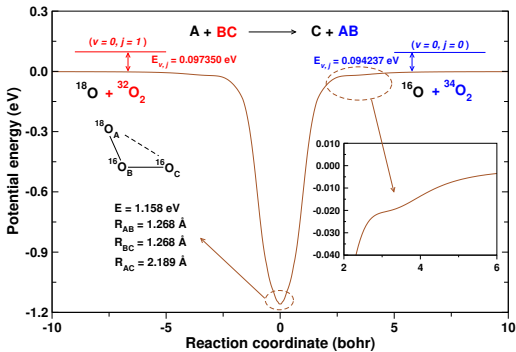
- ▶ TDWP method in energy range: 0.0 eV - 0.1 eV.
 - ▶ Only 8+66 isotopic variant of the reaction is investigated.
-

PES:

- ▶ Varga et al.¹ (*surface doesn't have the false submerged barrier.*)

¹ J. Chem. Phys., 147, 154312 (2017).

Energetics



- ▶ **8+66 reaction:**
Exoergic $\sim 0.003113 \text{ eV}$ (including ZPE of product and $(v = 0, j = 1)$ of reactant).
- ▶ Deep minima of energy 1.158 eV is present.
- ▶ No submerged reef (check inset figure).

Results: Total reaction probability

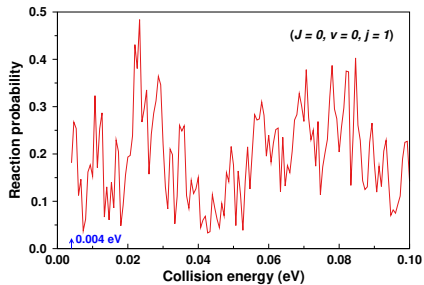


Figure 19: Total reaction probability at $J=0$.

Results: Total reaction probability

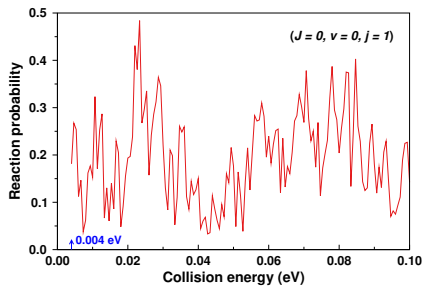


Figure 19: Total reaction probability at $J=0$.

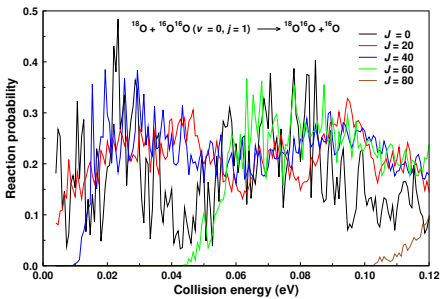


Figure 20: Total reaction probability at selected J .

Results: State-selected integral cross section

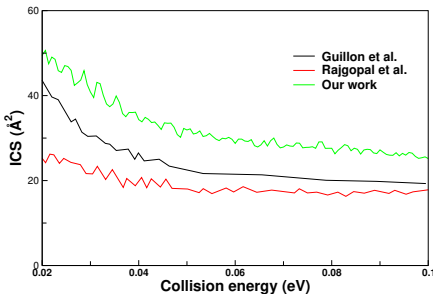
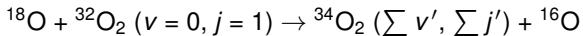


Figure 21: ICSs as a function of collision energy.

- ▶ ICS \downarrow as collision energy \uparrow .
- ▶ The three ICSs follow the same pattern.

Results: State-to-state ICS

Total energy: collision energy + $E_{v,j}$ of $^{32}\text{O}_2$ (0.09735 eV).

Results: State-to-state ICS

Total energy: collision energy + $E_{v,j}$ of $^{32}\text{O}_2$ (0.09735 eV).

Up to 0.1 eV of collision energy: Only **1 vibrational and 25 rotational levels** of product diatom.

Results: State-to-state ICS

Total energy: collision energy + $E_{v,j}$ of $^{32}\text{O}_2$ (0.09735 eV).

Up to 0.1 eV of collision energy: Only **1 vibrational and 25 rotational levels** of product diatom.

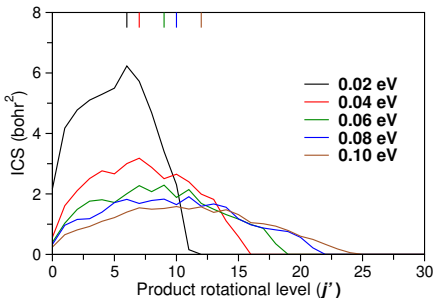


Figure 22: ICSs vs product rotational level (j'') at different collision energies.

Results: State-to-state ICS

Total energy: collision energy + $E_{v,j}$ of $^{32}\text{O}_2$ (0.09735 eV).

Up to 0.1 eV of collision energy: Only **1 vibrational and 25 rotational levels** of product diatom.

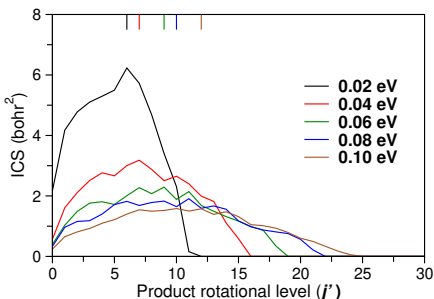


Figure 22: ICSs vs product rotational level (j') at different collision energies.

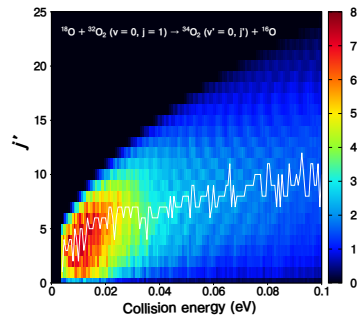


Figure 23: ICSs vs product rotational level (j') as a function of collision energies.

- ▶ Collision energy (\uparrow): ICS distributions become rotationally hot.
- ▶ Collision energy (\uparrow): broader range of j' .

Conclusion

Conclusion

General findings:

- ▶ Rich resonances are found in reaction probability and ICSs for the complete collision energy range of investigation.
 - ▶ ICSs follow the same behavior as the results reported earlier.
-

Conclusion

General findings:

- ▶ Rich resonances are found in reaction probability and ICSs for the complete collision energy range of investigation.
- ▶ ICSs follow the same behavior as the results reported earlier.

Scope of current work:

- ▶ Current work presents detailed TDWP investigation of 8+66 reaction variant.
 - ▶ Detailed dynamical insights about the reaction.
-

Conclusion

General findings:

- ▶ Rich resonances are found in reaction probability and ICSs for the complete collision energy range of investigation.
 - ▶ ICSs follow the same behavior as the results reported earlier.
-

Scope of current work:

- ▶ Current work presents detailed TDWP investigation of 8+66 reaction variant.
 - ▶ Detailed dynamical insights about the reaction.
-

Limitations:

- ▶ Computation time is the bottleneck: **Current QM calculations took ~ 23 years of computational time.**
- ▶ So, it is difficult to comment on thermal rate constants and isotopic effects using current calculations.



- ▶ Two different research themes: construction of PES and dynamics.
 - ▶ Chapter 3 and 4: Two pathways of LiH^+ destruction are investigated.
 - ▶ QCT methods are accurate enough for exoergic barrierless reaction system.
 - ▶ Chapter 5: Rigorous and accurate dynamics is performed for 8+66 variant of O_2 reaction.
-

¹ manuscript under preparation.



- ▶ Two different research themes: construction of PES and dynamics.
 - ▶ Chapter 3 and 4: Two pathways of LiH^+ destruction are investigated.
 - ▶ QCT methods are accurate enough for exoergic barrierless reaction system.
 - ▶ Chapter 5: Rigorous and accurate dynamics is performed for 8+66 variant of O_2 reaction.
-

What's next?

¹ manuscript under preparation.



- ▶ Two different research themes: construction of PES and dynamics.
 - ▶ Chapter 3 and 4: Two pathways of LiH^+ destruction are investigated.
 - ▶ QCT methods are accurate enough for exoergic barrierless reaction system.
 - ▶ Chapter 5: Rigorous and accurate dynamics is performed for 8+66 variant of $\text{O} + \text{O}_2$ reaction.
-

What's next?

- ▶ To construct the PESs for the molecular system with atoms >3.
- ▶ A few problems were encountered while using ML, which has to be perfected. Since ML methods are extremely helpful in constructing PES with large no. of atoms.
- ▶ Report the formation of LiH^+ on HeLiH^+ channel ¹.
- ▶ To investigate the origin of resonances observed in 8+66 reaction observables.

¹manuscript under preparation.

Acknowledgement



Supervisor:

Prof. Susanta Mahapatra

DRC members:

Prof. Debashish Barik and Dr. K. V. Jovan Jose

Dean School of Chemistry, UoH

Computing facilities:

Centre for Modelling Simulation and Design (CMSD)

UPE II, School of Chemistry, UoH

Funding:

UoH and DST

Lab mates, friends, and family

Visit:  <https://github.com/ajaymrawat/>

Thank you!



Additional slides

Chapter 2: Extras

Wavepacket propagation in Chebyshev approximation:

$$q^{J,\Omega'}(r_N, t + \Delta t) = 2\hat{H}_s q^{J,\Omega'}(r_N, t) - q^{J,\Omega'}(r_N, t - \Delta t) \quad (18)$$

$$q^{J,\Omega'}(t) = \hat{H}_s q^{J,\Omega'}(t - \Delta t) - \sqrt{1 - \hat{H}_s^2} p^{J,\Omega'}(t - \Delta t) \quad (19)$$

\hat{H}_s is scaled Hamiltonian and can be written as \hat{H} easily.

Chapter 2: Extras

Wavepacket propagation in Chebyshev approximation:

$$q^{J,\Omega'}(r_N, t + \Delta t) = 2\hat{H}_s q^{J,\Omega'}(r_N, t) - q^{J,\Omega'}(r_N, t - \Delta t) \quad (18)$$

$$q^{J,\Omega'}(t) = \hat{H}_s q^{J,\Omega'}(t - \Delta t) - \sqrt{1 - \hat{H}_s^2} p^{J,\Omega'}(t - \Delta t) \quad (19)$$

\hat{H}_s is scaled Hamiltonian and can be written as \hat{H} easily.

Hamiltonian for A+BC reaction system:

$$\begin{aligned} \hat{H} q^{J,\Omega'}(R_c, r_c, \gamma_c, t) = & -\frac{\hbar^2}{2\mu_{r_c}} \frac{\partial^2}{\partial r_c^2} q^{J,\Omega'}(R_c, r_c, \gamma_c, t) - \frac{\hbar^2}{2\mu_{R_c}} \frac{\partial^2}{\partial R_c^2} q^{J,\Omega'}(R_c, r_c, \gamma_c, t) \\ & + \left(\frac{1}{2I_{r_c}} + \frac{1}{2I_{R_c}} \right) \hat{j}^2 q^{J,\Omega'}(R_c, r_c, \gamma_c, t) + \frac{(\hat{J}^2 - 2\hat{J}_z \hat{j}_z)}{2I_{R_c}} q^{J,\Omega'}(R_c, r_c, \gamma_c, t) \\ & + \hat{V}_{elec} q^{J,\Omega'}(R_c, r_c, \gamma_c, t) - \frac{(\hat{J}_+ \hat{j}_- + \hat{J}_- \hat{j}_+)}{2I_{R_c}} q^{J,\Omega'}(R_c, r_c, \gamma_c, t) \end{aligned} \quad (20)$$

Action of different parts of Hamiltonian: carried out with different numerical methods.

Theory and Methodology: QM observables

► Reaction probability:

$$P_{vj}^J(E) = \sum_{\Omega=0}^j \frac{g_\Omega}{2j+1} \sum_{v'} \sum_{j'} \sum_{\Omega'} \frac{1 + \delta_{\Omega'0}}{2} \sum_{p=0}^1 |S_{v,j\Omega \rightarrow v'j'\Omega'}^{J,p}(E)|^2 \quad (21)$$

$$P_{vj}^J(E) = \sum_{\Omega} \frac{g_\Omega}{2j+1} \sum_{v'} \sum_{j'} \sum_{\Omega'} |S_{v,j\Omega \rightarrow v'j'\Omega'}^J(E)|^2 \quad (22)$$

$g_\Omega = 1$ for $\Omega = 0$ and $g_\Omega = 2$ for $\Omega > 0$.

► Cross section (ICS):

$$\sigma_{vj}(E) = \frac{\pi}{k_{vj}^2} \sum_{\Omega=0}^j \frac{g_\Omega}{2j+1} \sum_{J \geq \Omega}^{J_{\max}} (2J+1) \sum_{v'} \sum_{j'} \sum_{\Omega'}^{\min(J,j')} P_{vj\Omega \rightarrow v'j'\Omega'}^J(E) \quad (23)$$

The observables are state-selected. State-to-state observables can also be calculated.

Theory and Methodology: QM observables

► Rate Constant:

$$k_{vj}(T) = \sqrt{\frac{8k_B T}{\pi \mu_{A-BC}}} \frac{1}{(k_B T)^2} \int_0^{\infty} \sigma_{vj}(E) e^{-E/k_B T} E dE \quad (24)$$

► Differential cross section (DCS):

$$\sigma_{vj \rightarrow v'j'}^{\text{DCS}}(E, \theta) = \frac{1}{4k_{vj}^2} \sum_{\Omega=0}^j \left(\frac{g_{\Omega}}{2j+1} \right) \sum_{J \geq \Omega}^{J_{\max}} (2J+1) \sum_{\Omega'} |\mathcal{S}_{v,j\Omega \rightarrow v'j'\Omega'}^J(E) d_{\Omega\Omega'}^J(\pi - \theta)|^2 \quad (25)$$

Theory and Methodology: QCT observables

► Reaction probability:

$$P_{vj}^{\text{GB}}(E_{\text{col}}) = \frac{\sum_{i=1}^{N_r} w_i}{N} \quad P_{vj}^{\text{HB}}(E_{\text{col}}) = \frac{N_r}{N} \quad (26)$$

► Cross section (ICS):

$$\sigma_{vj \rightarrow v'j'}^{E_{\text{col}}} = \pi b_{\max}^2 P_{vj \rightarrow v'j'}(E_{\text{col}}) \quad (27)$$

► Rate constant:

$$k_{vj \rightarrow v'j'}(T) = \sqrt{\frac{8k_B T}{\pi \mu_{\text{A-BC}}}} \left(\frac{1}{k_B T}\right)^2 \int_0^\infty E_{\text{col}} \sigma_{vj \rightarrow v'j'}^{E_{\text{col}}} e^{-\frac{E_{\text{col}}}{k_B T}} dE_{\text{col}} \quad (28)$$

► Differential cross section (DCS):

$$\frac{d\sigma_{vj}(E_{\text{col}}, \theta)}{d\omega} = \frac{\sigma_{vj}^{E_{\text{col}}}}{2\pi} \left[\frac{1}{2} + \sum_{n=1}^M a_n P_n(\cos\theta) \right] \quad (29)$$

$$a_n = \frac{2n+1}{2} \frac{1}{\sum_{i=1}^{N_r} w_i} \sum_{i=1}^{N_r} P_n(\cos\theta_i)$$

Chapter 3: Extras

Isotopic effect: Mass-weighted PES

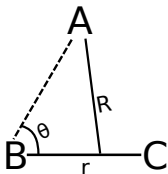
- ▶ Mass-weighted coordinates Q_1 and Q_2 are:

$$Q_1 = \sqrt{\mu_{A-BC}} R \quad (30)$$

$$Q_2 = \sqrt{\mu_{BC}} r \quad (31)$$

- ▶ Skew angle (β)

$$\beta = \cos^{-1} \left(\sqrt{\frac{m_A m_C}{(m_B + m_C)(m_A + m_B)}} \right) . \quad (32)$$



Q_1 and Q_2 are connected with R and r , respectively.

Chapter 3: Extras

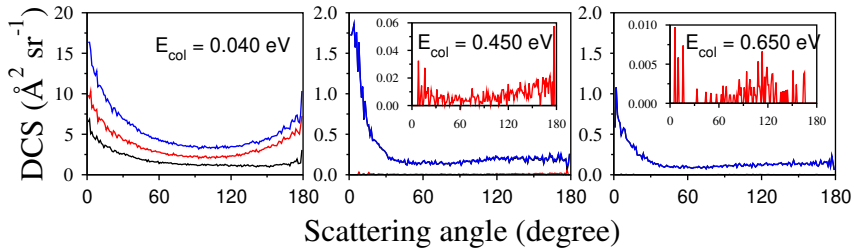


Figure 24: Direct and indirect DCSs for R1 and R2.

Chapter 4: Extras

Comparing fitted and ab initio data

Global minima:

Parameters of global minima	This work	ab initio values
$R_{\text{LiHe}^+} (a_0)$	3.636	3.650
$R_{\text{LiH}^+} (a_0)$	4.192	4.191
$R_{\text{HeH}} (a_0)$	7.829	7.841
$\angle \text{HeLiH}^+$	180°	180°
E (eV)	-0.2038	-0.2034

Chapter 4: Extras

Comparing fitted and ab initio data

Global minima:

Parameters of global minima	This work	ab initio values
R_{LiHe^+} (a_0)	3.636	3.650
R_{LiH^+} (a_0)	4.192	4.191
R_{HeH} (a_0)	7.829	7.841
$\angle \text{HeLiH}^+$	180°	180°
E (eV)	-0.2038	-0.2034

Diatomlic minima:

	R_{eq} (a_0)	E_{eq} (eV)
LiHe⁺		
This work	3.638	-7.509E-2
Wernli et al.	3.586	-7.965E-2
ab initio data	3.641	
LiH⁺		
This work	4.183	-0.1325
Wernli et al.	4.142	-0.1380
ab initio data	4.186	

Chapter 5: Extras

Different PESs for O₃

2001	R. Siebert, R. Schinke, and M. Bittererova. Spectroscopy of Ozone at the Dissociation Threshold: Quantum Calculations of Bound and Resonance States on a New Global Potential Energy Surface. <i>Phys. Chem. Chem. Phys.</i> 3, 1795 (2001).
2003	P. Fleurat-Lessard, S. Y. Grebenschikov, R. Siebert, R. Schinke, and N. Halberstadt. Theoretical Investigation of the Temperature Dependence of the O + O ₂ Exchange Reaction. <i>J. Chem. Phys.</i> 118, 610 (2003).
2003	D. Babikov, B. K. Kendrick, R. B. Walker, R. T. Pack, P. Fleurat-Lesard, and R. Schinke. Metastable States of Ozone Calculated on an Accurate Potential Energy Surface. <i>J. Chem. Phys.</i> 118, 6298 (2003).
2004	R. Schinke and P. Fleurat-Lessard. The transition-state region of the O + O ₂ potential energy surface. <i>J. Chem. Phys.</i> 121, 5789 (2004).
2010	Hernández-Lamoneda, Michael R. Salazar, and R.T. Pack. Does ozone have a barrier to dissociation and recombination? <i>Chem. Phys. Lett.</i> 355, 478 (2002).
2010	Filip Holka, Péter G. Szalay, Thomas Müller, and Vladimir G. Tyuterev. Toward an Improved Ground State Potential Energy Surface of Ozone. <i>J. Phys. Chem. A</i> 114, 9927 (2010).
2011	Dawes, R.; Lolur, P.; Ma, J.; Guo, H. Highly Accurate Ozone Formation Potential and Implications for Kinetics. <i>J. Chem. Phys.</i> 135, 081102 (2011).
2013	M. Ayouz and D. Babikov. Global permutationally invariant potential energy surface for ozone forming reaction. <i>J. Chem. Phys.</i> 138, 164311 (2013).
2013	V. G. Tyuterev, R. V. Kochanov, S. A. Tashkun, F. Holka, and P. Szalay. New Analytical Model for the Ozone Electronic Ground State Potential Surface and Accurate ab initio Vibrational Predictions at High Energy Range. <i>J. Chem. Phys.</i> 139, 134307 (2013).
2013	R. Dawes, P. Lolur, A. Li, B. Jiang, and H. Guo. An Accurate Global Potential Energy Surface for the Ground Electronic State of Ozone. <i>J. Chem. Phys.</i> 139, 201103 (2013).
2017	Z. Varga, Y. Paukku, and D. G. Truhlar. Potential energy surfaces for O + O ₂ collisions. <i>J. Chem. Phys.</i> 147, 154312 (2017).

Chapter 5: Extras

8+66 ICS from 0.01 - 0.1 eV

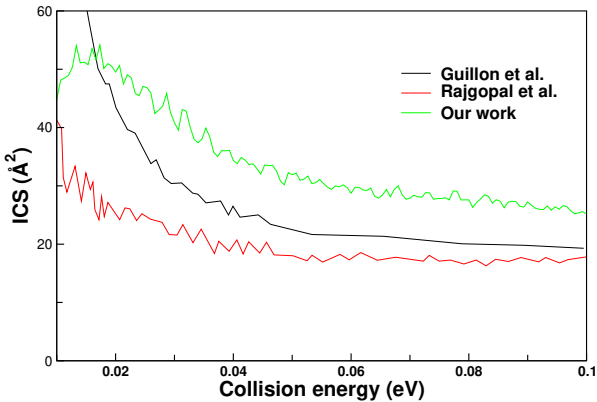


Figure 25: ICS for 8+66 reaction.